Biochimica et Biophysica Acta 1847 (2015) 379–389

Contents lists available at ScienceDirect

Biochimica et Biophysica Acta

journal homepage: www.elsevier.com/locate/bbabio

Photoinduction of cyclosis-mediated interactions between distant chloroplasts

Alexander A. Bulychev *, Anna V. Komarova

Department of Biophysics, Faculty of Biology, Moscow State University, Moscow 119991, Russia

ARTICLE INFO

Article history:
Received 10 October 2014
Received in revised form 10 January 2015
Accepted 13 January 2015
Available online 20 January 2015

Keywords:
Induction phenomena
Intracellular communications
Long-distance signaling
Cytoplasmic streaming
Patterned illumination
Methyl viologen

ABSTRACT

Communications between chloroplasts and other organelles based on the exchange of metabolites, including redox active substances, are recognized as a part of intracellular regulation, chlororespiration, and defense against oxidative stress. Similar communications may operate between spatially distant chloroplasts in large cells where photosynthetic and respiratory activities are distributed unevenly under fluctuating patterned illumination. Microfluorometry of chlorophyll fluorescence in vivo in internodal cells of the alga *Chara corallina* revealed that a 30-s pulse of localized light induces a transient increase (~25%) in F' fluorescence of remote cell parts exposed to dim background light at a 1.5-mm distance on the downstream side from the illuminated spot in the plane of unilateral cytoplasmic streaming but has no effect on F' at equal distance on the upstream side. An abrupt arrest of cytoplasmic streaming for about 30 s by triggering the action potential extended either the ascending or descending fronts of the F' fluorescence response, depending on the exact moment of streaming cessation. The response of F' fluorescence to localized illumination of a distant cell region was absent in dark-adapted internodes, when the localized light was applied within the first minute after switching on continuous background illumination of the whole cell, but it appeared in full after longer exposures to continuous background light. These results and the elimination of the F' response by methyl viologen known to redirect electron transport pathways beyond photosystem I indicate the importance of photosynthetic induction and the stromal redox state for long-distance communications of chloroplasts in vivo.

1. Introduction

Communications of chloroplasts with other cell compartments are essential for photosynthesis since they enable continuous exchange of metabolites and eventual export of assimilates [1,2]. They are also involved in the regulation of photosynthetic electron flow by adjusting the electron flux to demands and capacity of the carbon assimilation cycle for utilizing ATP and NADPH [3,4]. A great deal of attention has been paid to metabolic interactions of chloroplasts and mitochondria [5–9]. Beneficial cooperation of respiratory and photosynthetic metabolism is evidenced, for example, by colocalization of chloroplasts and mitochondria during repositioning of plastids in vivo under variations in irradiance [10]. In internodal cells of characean algae, known for their ability to generate alternate photosynthetically active and inactive bands, the cortical mitochondria relocate after dark–light transition by moving from cell regions with low photosynthetic activity to high activity regions [11]. The chloroplast–cytosol–mitochondria interactions are largely due to the exchange of redox equivalents mediated by metabolic transporters located in the envelope membranes [6,12,13]. The malate/oxaloacetate shuttle plays a principally important role in rapid redox balancing within the chloroplast stroma [4].

Much less attention has been given to interchloroplast communications, even though chloroplast functioning can be affected by neighboring and distant green plastids through cytoplasmic concentrations of shared substrates and products of their metabolism, such as reducing equivalents, including NAD(P)H. These interactions are particularly interesting in the context of long-distance signaling in large cells where intracellular concentration gradients arise under uniform and nonuniform distribution of irradiance or other external factors. Characean algae are able to generate under light the contrast patterns of external pH, calcification, CO_2 and O_2 content, as well as the patterns of photosynthetic electron-transport rates, non-photochemical quenching, and probably cytoplasmic pH [14,15]. Although uniform illumination is sufficient for pattern emergence, the spot illumination resembling sunflecks of natural fluctuating daylight was found to promote zonation of photosynthesis and external pH. Large changes in chlorophyll fluorescence F_m' (emission induced by saturating light pulses) and external pH at a distance from the illuminated spot occurred rapidly after lag periods of about 1–2 min from the onset of localized illumination [16].

Abbreviations: AP, action potential; DPI, diphenyleneiodonium; LL, localized light (pulse); FNR, ferredoxin–NADP reductase; MV, methyl viologen; PFD, photon flux density; pH_o, pH in the outer medium near the cell surface; PSI and PSII, photosystems I and II

* Corresponding author. Tel.: +7 495 939 3503; fax: +7 495 939 1115.
E-mail addresses: bulychev@biophys.msu.ru (A.A. Bulychev), ava1945@mail.ru (A.V. Komarova).

http://dx.doi.org/10.1016/j.bbabio.2015.01.004
0005-2728/

Dynamic variations of photosynthetic activity in seemingly uniform cell parts, located away from the brightly illuminated spot, imply the propagation of some photoinduced signal.

Measurements of chlorophyll fluorescence and surface pH on microscopic regions of *Chara corallina* internodes revealed that the signal transmission along the cell is clearly vectorial; the asymmetry of propagation is determined by the direction of cytoplasmic streaming in the plane of measurements [17,18]. The transient changes of surface pH and F_m' in cell regions around the narrow light spot occurred only on the downstream side with respect to the direction of streaming, while no changes were observed on the upstream side from the point of illumination. The cytoplasmic flow is thus an important means for long-distance transmission of signals in giant cells. The signal is generated in brightly illuminated anchored chloroplasts, transferred downstream from the source area with the cytoplasmic flow, and is perceived by the remote photosynthetic organelles and plasmalemmal transporters exposed to dim light [18]. The supposed role of cyclosis in intracellular communications [19] thus receives an experimental support.

The mechanisms and functions of rotational streaming in plant cells were considered in several reviews [20–22]. The cytoplasmic streaming (cyclosis) is based on ATP-dependent movement of myosin molecules along the actin microfibrils. The myosin molecules carry the attached vesicles, whose movement entrains the liquid flow. The velocity of cytoplasmic streaming in *Chara* could be as high as 100 μm/s. The streaming is sensitive to cytoplasmic Ca^{2+} and stops immediately when the Ca^{2+} level increases dramatically during the action potential [23,24]. The streaming recommences in parallel with the decrease in cytoplasmic Ca^{2+} in about 30 s after the action potential and restores completely within 5–10 min.

The cyclosis-mediated long-distance interchloroplast communications were earlier noted from measurements of F_m' fluorescence (maximal chlorophyll fluorescence induced by saturating light pulses) in *Chara* internodes [17]. Following localized illumination of a remote cell region, the F_m' was strongly quenched in the cell area unexposed to spot light; this quenching developed after lag periods increasing linearly with the distance between the illuminated and analyzed areas. Subsequent studies revealed that the shape and extent of F_m' changes in response to a localized light stimulus depend on the background irradiance of the whole cell [25]. The F_m' quenching after illumination of a remote cell region developed at moderate intensities of background light, while the increase in F_m' was observed at low intensities. Comparison of the parameters F_m' and F_m (F_m is the maximal fluorescence of a dark-adapted sample) provides a suitable measure of non-photochemical quenching [26]. The properties of F_m' changes induced by localized illumination of remote cell parts have been characterized recently [25]. By contrast, the effects of localized light pulses on actual chlorophyll fluorescence in distant cell parts remained scarcely examined. However, the actual fluorescence designated as F or F' [26,27] contain primary information on the extent of photochemical quenching (qP) determined by the oxidoreduction state of the quinone acceptor Q_A in the photosystem II (PSII) [28,29].

The actual fluorescence F' of microscopic cell areas can be recorded continuously, so that much more data are sampled per unit time compared to F_m'. The resolution of F_m' measurement in the Microscopy–PAM system (Walz) is limited by temporal spacing of saturation light pulses (10–20 s) [30]. The resolution of F' measurements is also limited because of very low irradiance employed for assaying F_o (fluorescence of a dark-adapted cell) on areas of microscopic dimensions. Thus, a satisfactory signal-to-noise ratio is achieved by means of signal damping, which sets limits on temporal resolution. Continuous recording of F' might serve a valuable supplement to the complete measurements of F' and F_m' with repetitive saturating light pulses.

The multiphasic fluorescence transients in continuous light, known as the fluorescence induction, are related to the induction phenomena in photosynthesis. The photosynthetic induction was formerly concluded from inability of dark-adapted leaves to commence CO_2 fixation immediately on illumination, in contrast to preilluminated leaves where assimilation started immediately [31]. The phenomena of photosynthetic induction have multiple other manifestations, including different kinetics of P700 redox state and thylakoid membrane potential upon illumination of dark-adapted and preilluminated samples [32,33].

The aim of this study was to examine the effect of localized illumination of a distant cell part on actual fluorescence F' under actinic light in order to trace possible influence of cyclosis-transported metabolites, specifically reducing equivalents, on the redox state of electron-transport chain on the acceptor side of PSII. To this end, we employed microfluorometry of *Chara* chloroplasts in vivo and applied localized illumination to cell regions located upstream the cytoplasmic flow at a millimeter-scale distance from the analyzed area. The results show that spot illumination is followed by a large transient increase in fluorescence F' in the remote cell area and that the photoinduced signal is transmitted by the streaming cytoplasm. Furthermore, the fluorescence F' of "recipient" chloroplasts was found to be insensitive to the transported signal at the initial stages of the photosynthetic induction and become fully sensitive after the induction period of few minutes.

2. Materials and methods

2.1. Plant material

C. corallina algae were grown in an aquarium at room temperature at scattered daylight (photosynthetic photon flux density ~10 μmol m^{-2} s^{-1} during daytime). Isolated internodal cells measuring 6–8 cm in length and about 0.9 mm in diameter were placed into artificial pond water containing 0.1 mM KCl, 1.0 mM NaCl, and 0.1 mM $CaCl_2$. The medium was supplemented with $NaHCO_3$ to adjust the pH at 7.0. Prior to experiments the cell was mounted in a transparent organic glass chamber with a total bath volume of 40 mL and placed on a stage of an inverted fluorescence microscope Axiovert 25-CFL (Zeiss, Germany).

2.2. Continuous and pulse-amplitude-modulated microfluorometry

Parameters of chlorophyll fluorescence in vivo were measured on microscopic cell regions (diameter ~100 μm) using a Microscopy–PAM fluorometer (Walz, Germany) equipped with a ×32/0.4 objective lens. Data represent changes in actual fluorescence F' emitted under background illumination of the whole cell and changes in maximal fluorescence F_m' induced by saturating light pulses. The frequency of modulated measuring light was usually set at ~40 Hz.

The counter-directed cytoplasmic flows in *Chara* internodes occur on diametrically opposite cell sides that are separated by distances up to 900–1000 μm. The cytoplasmic layer, about 10 μm thick, comprises the immobile ectoplasm with tightly packed rows of chloroplasts and the streaming endoplasm. At a sufficiently high numerical aperture of the objective lens, the depth of field does not exceed few micrometers. Therefore, fluorescence can be selectively measured for chloroplasts residing on the lower cell side where the direction of streaming is well defined.

The signal from a photomultiplier was fed into the PAM Control Unit of pulse-amplitude modulation system, digitized by means of an AD converter PCI-6024E (National Instruments, United States), and displayed on a computer monitor using WinWCP program (Strathclyde Electrophysiology Software). Data points were sampled at regular intervals of about 51 ms.

The OJIP fluorescence induction curves were measured with the plant efficiency analyzer (PEA, Hansatech, United Kingdom) using test tubes containing about 20 internodal cells. This fluorometer allowed measurements of time-resolved fluorescence induction in the time range form 50 μs to 250 s.

2.3. Background and localized illumination

The excitation/emission light beams used for microfluorometry, the position of an optic fiber employed for localized photostimulation of a distant cell area, and the background illumination of the whole internode were configured as shown schematically in a previous work [25].

The background illumination of the whole cell was provided from the microscope upper light source through a 5-mm thick blue glass filter SZS-22 ($\lambda < 580$ nm). The incident photon flux density (PFD) from this light source was determined with a Spherical Micro Quantum Sensor US-SQS connected to a PAM Control Unit (Walz). The intensity of background illumination was attenuated by neutral density glass filters. In the major part of experiments, the PFD incident on the upper cell side was approximately 9 μmol m^{-2} s^{-1}. The upper chloroplast layer transmitted about one-third of the incident flux, providing irradiance ~3 μmol m^{-2} s^{-1} at the chloroplast bottom layer. In some experiments the cell part comprising the area of localized illumination was screened from background light. This was accomplished by placing 6-mm wide plates above and under the cell to screen the cell part from incident and reflected light.

The localized illumination (localized light, LL) was applied through a thin quartz optic fiber to a cell region at a distance $d =$ 1.5 mm from the point of measurements. The optic fiber with a diameter of 400 μm was connected to a source of white light (a light-emitting diode Luxeon LXK2-PWN2-S00, Lumileds, United States). The PFD at the output of the light guide was 500 μmol m^{-2} s^{-1} [17]. In order to reduce the number of intermediates exchanged between the chloroplasts and cytoplasm in the area of localized illumination, comparatively short (30 s) pulses of LL were used in most experiments. In this case the cytoplasmic composition is modulated by rapidly exchanging components. For the purpose of comparison we used also LL pulses ranging from 2.5 to 170 s. The free end of the light guide was fixed in the holder of a mechanical KM-1 micromanipulator (Chernogolovka, Russia) under the angle of 30–45° to a horizontal plane. After adjusting the light guide position in the view field near the cell, the optic fiber was displaced with a micrometric screw to a 1.5-mm distance upstream the cytoplasmic flow with respect to the analyzed region.

2.4. Measurements of surface pH at rest and after membrane excitation

The local pH on the outer cell surface (pH_o) was measured with glass-insulated antimony pH-microelectrodes having tip diameters of 5–15 μm. The slope of the electrode function was about 54 mV/pH unit. The tracking pH_o provided a convenient mark for the action potential generation and allowed us to identify the cell regions with active H^+ extrusion (pH_o 6.2–6.7) and the areas of passive H^+ inflow (pH_o 8–10). The experiments were usually performed in the acidic areas that are free of calcium incrustations, even in mature cells.

The action potential (AP) generation and the immediate arrest of cytoplasmic streaming were triggered by passing a short pulse of transcellular electric current (10 μA, 150 ms). The electrodes used for this purpose were isolated from the pH-measuring circuit; they were placed in electrically insulated compartments of the experimental chamber. The streaming in *Chara* cells reappears in about 30 s after the AP generation and attains its maximal velocity within about 10 min [23,34]. The velocity of cyclosis was determined in the transmitted light before the onset of fluorescence measurements. Streaming velocities were usually 70–90 μm/s.

The chloroplast fluorescence is sensitive to the AP generation, the response amplitude being dependent on the irradiance and the direction of H^+ transport in analyzed areas [35]. Considering this circumstance, low intensities of background illumination were used to minimize the AP-induced fluorescence shifts.

2.5. Measurements of P700 redox transients

The induction phenomena in photosynthesis comprise activation of ferredoxin–NADP reductase (FNR) whose activation status is manifested in the kinetics of P700 photooxidation [33]. Redox transients of P700 chlorophyll in PSI reaction centers were measured from changes in the absorbance difference at 810 and 870 nm (ΔA_{810}) [36]. The measuring system consisted of a PAM-101 control unit (100 kHz modulation frequency) and ED-P700DW dual-wavelength emitter–detector unit (Walz, Germany). A multi-branch fiber-optic cable was used to guide modulated measuring beam and actinic light toward a *Chara* sample comprising about ten internodal cells aligned parallel and to direct transmitted infrared light toward the detector. The sample was placed between the reflecting mirror and the end of the fiber-optic cable. The cells were illuminated with white light of a Luxeon LXK2-PWN2-S00 light-emitting diode (Lumileds, United States) through a neutral density glass filter. The acquisition of ΔA_{810} signals and the timing control of light pulses from LED source were carried out by means of a PCI-6024E analog–digital (AD/DA) convertor (National Instruments, United States) and WinWCP software (Strathclyde Electrophysiology Software).

Methyl viologen was obtained from Acros Organics (Belgium). Diphenylene iodonium (Sigma) dissolved in DMSO (5 mg/mL) was a gift from Dr. N.P. Matveyeva (Moscow State University). The final concentration of the solvent in the bath solution was 0.06%, which had no effect on its own on photosynthesis and cytoplasmic streaming.

Data in figures show results obtained at least in triplicate with different cells. The averaged curves of fluorescence are presented, with the number of replicate measurements (n) specified in figure captions.

3. Results and interpretation

3.1. Cyclosis-mediated changes of chlorophyll fluorescence F′ in dim light

Fig. 1 shows the influence of localized illumination (a 30-s pulse of LL) on chlorophyll fluorescence of cell regions exposed to continuous dim light and located on the upstream and downstream sides from the illuminated area in the plane of cytoplasmic flow (curves *1* and *2*, respectively). When fluorescence was measured at a 1.5-mm distance

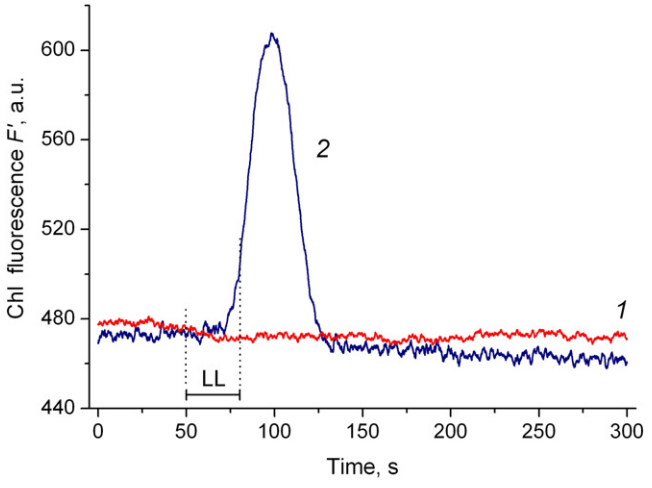

Fig. 1. Asymmetric propagation of chlorophyll fluorescence changes induced by localized illumination (localized light, LL) of cell areas positioned at a 1.5-mm distance from the fixed area of fluorescence measurement: (*1*) the lack of F' changes when the optic fiber illuminated the cell region positioned downstream in the cytoplasmic flow from the area of F' measurement; (2) a transient increase in F' when the tip of optic fiber was placed upstream from the analyzed area. The 30-s pulse of LL was applied at $t = 50$ s. Dotted lines and the bar labeled LL mark the period of localized illumination. The intensity of continuous background light was 9 μmol quanta m^{-2} s^{-1}. Traces *1* and *2* are average records obtained from replicate measurements on one cell ($n = 5$ and 2, respectively).

d from the center of illuminated area having a diameter of 0.4 mm, the parameter *F*′ underwent no changes on the upstream side (curve *1*) but exhibited a large (by about 25%) transient increase on the downstream side where the cytoplasmic flow arrived from the irradiated region. In the case of a 30-s pulse of LL and a 1.5-mm separation distance *d*, the major part of fluorescence *F*′ transients developed after turning off the LL. The signal shape fit well to the Gaussian curve, with the coefficient of determination R^2 up to 0.99. The Gaussian profile of the curves reflects their similarity to chromatographic peaks, because the metabolic signal released from chloroplasts in the region of intense local illumination moved with the cytoplasmic flow, passing by the area of measurements.

Unlike the time-shifted oppositely directed stages in the F_m' response to LL (a small increase followed by a large decrease in F_m') [25], the fluorescence increase was always the dominant component in the response of *F*′. Owing to the large number of data points in the records, the position of the peak and the width of the Gaussian curve are determined with an accuracy of better than 0.1 s. The results indicate that the transient increase in *F*′ is caused by the arrival of some photosynthetically active signal that was released in the area of localized illumination (source region), transmitted with the streaming fluid, and perceived by chloroplasts in cell regions exposed to dim background illumination (sink regions). In subsequent experiments only appropriate (upstream) position of the light guide was used.

Fig. 2A displays cyclosis-mediated fluorescence transients induced by LL pulses of various durations. The extension of the LL pulse from 30 to 100 s elevated the amplitude of *F*′ response, whereas the prolongation of pulse length to 170 s produced no additional increase. Unlike the roughly symmetrical shape of the *F*′ changes in response to a 30-s LL pulse, the kinetics of *F*′ changes induced by longer pulses was not symmetrical. After reaching the peak value in about 70 s from the onset of localized photostimulation, fluorescence started lowering. If this lowering reflects reoxidation of Q_A (increase in qP), it might be due to the decrease in concentration of the active metabolite in the streaming cytoplasm during prolonged illumination or to the appearance in the flow of an additional metabolite counteracting the increase in *F*′. Previous studies of cyclosis-mediated F_m' changes and H_2O_2 transfer in *Chara* cells pointed to the complex origin of transmitted signals [25,37].

Fig. 2B (curve *1*) shows the extent of cyclosis-mediated *F*′ changes (Δ*F*′) as a function of duration of the localized light pulse. The half-maximal response was observed at pulse durations of ~20 s. Curve *2* in Fig. 2B shows the results of similar experiments except that the "source" cell part exposed to localized lighting was screened from incidence of background light. We reasoned that the chloroplast functioning and cytoplasmic levels of light-dependent metabolites in the area of localized illumination might vary depending on preincubation of the cell in darkness or in background light. Specifically, the malate shuttle ensuring the transfer of reducing equivalents across the chloroplast envelope is under the control of the thioredoxin system and becomes activated on a dark-to-light transition [3,4]. The sigmoid shapes of curves *1* and *2* were similar, except that the response saturation was observed at longer light pulses in the case of screening the source part of the cell. It is possible that the cytoplasmic level of the signaling metabolite was lower in darkness than under background light and, accordingly, the signal level increased slower during localized illumination of the darkened cell part. In addition, the shift between curves *2* and *1* might be also due to the time delay required for activation of the photosynthetic metabolism after dark–light transition in chloroplasts exposed to LL.

3.2. Effects of interrupted streaming on cyclosis-mediated fluorescence changes

The involvement of cyclosis in fluorescence changes elicited by illumination of a distant cell region was further checked by combining the

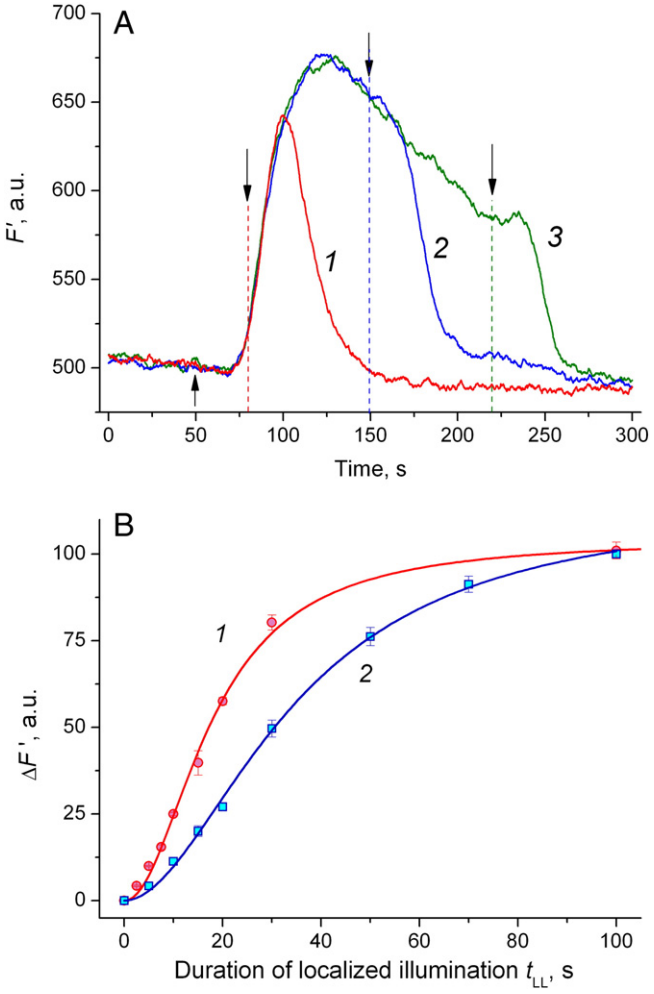

Fig. 2. Cyclosis-mediated fluorescence changes elicited by pulses of localized light of various durations. (A) Fluorescence responses to pulses of LL with duration of: (1) 30 s, (2) 100 s, and (3) 170 s. The upward arrow marks the onset of localized illumination; dashed lines and downward arrows indicate the moments when the localized light was switched off. Data are averaged records with $n = 5$, 4, and 4 for traces 1, 2, and 3, respectively. (B) Amplitude of fluorescence changes (Δ*F*′) as a function of the length of the LL pulse. (1) Under background illumination of the whole cell; (2) the cell part around the optic fiber was screened from incidence of continuous background light with a 6-mm wide shield. Data are mean values ± SE ($n = 3$–5).

LL treatment with the temporal cessation of cytoplasmic streaming. The streaming can be instantly arrested for about 30 s at any moment by triggering the AP generation. The AP is a transient large-scale depolarization of the plasma membrane occurring in the time frame of 2–3 s; it is negligibly short compared to the time range of fluorescence measurements (200–300 s). Fig. 3A shows *F*′ changes induced by a 60-s pulse of LL in the resting cells with continuous cytoplasmic streaming (curve *1*) and in the same cells after the temporal arrest of streaming at the moment coincident with the onset of localized illumination (curve *2*). In the case of uninterrupted streaming, the slopes of the front and rear parts of the *F*′ response were nearly equal, except that these slopes were positive and negative, respectively.

When the AP causing the immediate arrest of cyclosis was elicited synchronously with the onset of LL, the profile of the *F*′ response shifted its peak to longer times (by ~50 s) and acquired a clearly asymmetric shape (curve *2*). In this case continuous outflow of the signaling substance from brightly illuminated zone was stopped temporally; the transport across the chloroplast envelope membrane proceeded in the stagnant environment, and the arrival of signal to the area of measurements was postponed until the restoration of cytoplasmic streaming. The slope of the rear front in the *F*′ response was similar to that in the

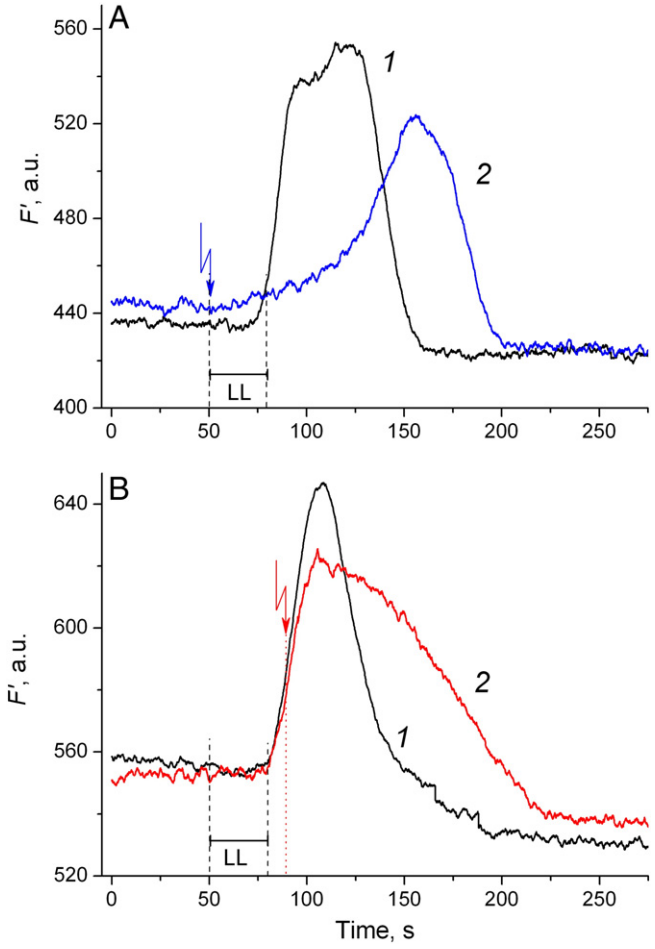

Fig. 3. Effects of the temporal arrest of cytoplasmic streaming on cyclosis-mediated changes of actual fluorescence F'. (A) Fluorescence changes induced by a 60-s pulse of LL in the resting cells with continuous cytoplasmic streaming (curve *1*) and in the same cells after temporal arrest of streaming at the moment $t = 50$ s (curve *2*). Dashed lines and a bar labeled LL mark the interval of localized illumination; the zigzag arrow indicates the moment when the action potential was elicited and caused the immediate arrest of streaming for about 30 s. Curves *1* and *2* are averaged records for $n = 4$ and 3, respectively. (B) Fluorescence changes induced by a 30-s pulse of localized illumination in the resting cell with continuous cytoplasmic streaming (curve *1*) and in the same cell after temporal arrest of streaming by eliciting the action potential at the moment indicated with a zigzag arrow (curve *2*). Curves *1* and *2* are averaged records for $n = 10$ and 5, respectively.

resting cell, whereas the steepness of the leading slope increased gradually and was much lower than in an unexcited (resting) cell. The gradual increase in steepness of the rising front seems to reflect the restoration and acceleration of cytoplasmic streaming. The amplitude of the F' peak after the AP generation (curve *2*) was lower than in the resting cell (curve *1*) indicating that the stagnant cytoplasm did not accumulate large amounts of the transportable metabolite during the arrest of streaming. Similar slopes of the F' decline after the 60-s light pulse under normal and interrupted cyclosis indicate that the velocities of cytoplasmic streaming approached the initial values in about 2 min after the AP generation.

Fig. 3B shows the kinetics of F' changes in response to the 30-s pulse of LL when cyclosis was undisturbed (curve *1*) or arrested at the rising stage of F' changes (curve *2*). In the latter case, the photoinduced cytoplasmic signal was expected to stop its movement, together with the liquid flow, at the moment of passage through the analyzed area. The cessation of streaming at this stage did not affect the rising slope of the F' signal but strongly delayed and decelerated its descending slope. The F' response was asymmetric but the asymmetry was clearly different from that shown in Fig. 3A (curve *2*). The deceleration of the rear front is conceivable, because the physiologically active intermediate remained longer in the area of measurements after cessation of cytoplasmic streaming. The results show that the cessation of streaming modulates the fluorescence response in different ways depending on the precise moment of the cyclosis interruption. These variable profiles of F' changes reflect different dynamics of the signal passage across the area of fluorescence measurement depending on whether the cytoplasmic redox signal reached or did not reach the point of F' measurement on the moment of sudden stoppage of cytoplasmic streaming. In addition, the exchange of metabolites across the chloroplast envelope could be modulated in the standing cytoplasm.

3.3. Photoinduction of cyclosis-mediated fluorescence response

Fig. 4A shows the fluorescence records observed during sequential application of two pulses of localized light, LL_1 and LL_2. It is seen that the first 30-s pulse of LL applied to the cell shortly after 5-min dark incubation produced no fluorescence changes (the bar labeled LL_1 between dashed lines at $t = 50$ and 80 s marks the first period of localized illumination). By contrast, the application of the second identical pulse (LL_2 in the period from $t = 350$ to 380 s) produced a large transient increase in fluorescence peaking in about 50 s after the onset of localized illumination. Thus, the fluorescence responses to LL were absent in dark-adapted cells and appeared after preillumination for a few minutes with the background light. Clearly, a certain induction period was needed for the response development.

It is seen in Fig. 4A that the F' transient in response to the second pulse of LL was preceded by a slow increase and decrease of fluorescence (time span from 200 to 350 s). These changes of emission should not be considered as a delayed and diminished response to the first pulse of LL. As Fig. 4B (curve *1*) shows, a similar wave of fluorescence changes was observed during the cell exposure to dim background light without preceding application of LL pulse. The slow increase in F' under the action of continuous background light appears to be a part of the fluorescence induction curve observed under low intensity of incident light.

The intensity of background illumination at the bottom layer of chloroplasts in vivo was estimated at 3 μmol m^{-2} s^{-1} under assumption that the upper layer of chloroplasts attenuated the transmitted light by a factor of 3 in the peak of chlorophyll absorption. The slow induction of chlorophyll fluorescence under weak light is characterized much less in the literature than the fast stages of the induction kinetics in bright light [38]. Measurements of the fluorescence induction in *C. corallina* using Plant Efficiency Analyzer (PEA, Hansatech) indicated that the first fluorescence peak P was attained within less than 1 s after switching on red light at PFD ranging from 90 to 3000 μmol m^{-2} s^{-1} (Supplemental Fig. 1A). Hence, the fluorescence peak induced by dim background light and observed after 200-s illumination is likely to represent the intermediary peak M [38] or the peak M_2 described for *Bryopsis* [39].

The induction curves of F' fluorescence recorded with a Microscopy–PAM fluorometer on microscopic regions of *C. corallina* cells are shown in Supplemental Fig. 1B. It is seen that elevation of light intensity from 9 to 35 μmol m^{-2} s^{-1} was accompanied by the shift of the delayed peak of F' from t ~400 to 450 s to about 250 s. At low irradiance the delayed peak of F' developed in parallel with a small decrease in F_m', providing evidence that the decrease in photochemical quenching (qP) occurred concurrently with a slight increase in non-photochemical quenching (Supplemental Fig. 1C).

A similar pattern of F' and F_m' changes induced by continuous background illumination is also seen in Fig. 4B at $t = 200$–350 s (curves *1* and *2*). Thus, the increase in F' at this stage reflects the transient reduction of the acceptor Q_A and cannot be ascribed to the release of non-photochemical quenching. A similar reduction of Q_A (decrease in qP) during the SM transient in the fluorescence induction curves at low irradiance was assumed previously [38].

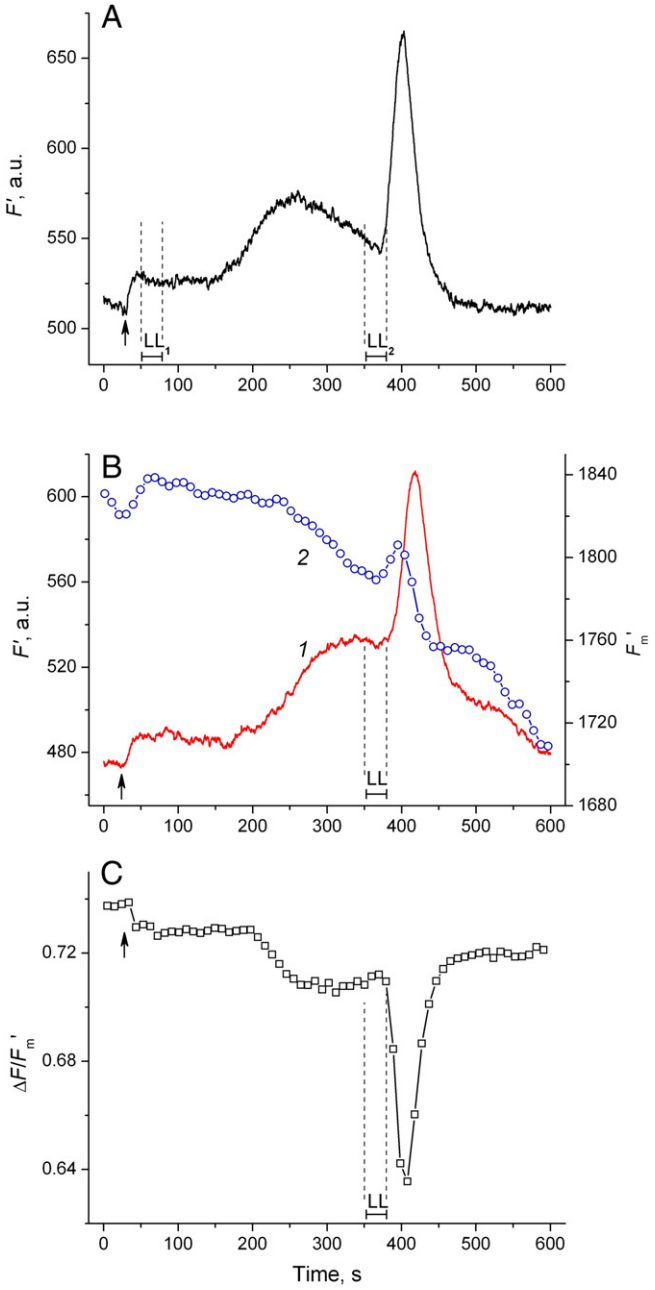

Fig. 4. Light-dependent induction of the F' response to localized illumination of a distant cell area in dark-adapted *C. corallina* internode. (A) The lack of the F' response to the first 30-s pulse of localized light (LL_1) after 5-min dark adaptation and full development of the F' response to the identical light pulse (LL_2) after 5.5 min of continuous background illumination. The upward arrows in this and other panels mark the onset of the background light (9 μmol quanta m^{-2} s^{-1}). Dashed lines and bars show the first (LL_1) and the second (LL_2) periods of localized illumination. The curve is an averaged record for $n = 3$. (B) Induction of cyclosis-mediated F' response under background light is independent on preillumination with the localized light pulse. Curve *2* with symbols represents the changes in maximal fluorescence F_m'. Dashed lines and a horizontal bar designate the beginning and end of a single LL pulse applied in 5.5 min after the onset of background illumination. Curves *1* and *2* are averaged records for $n = 4$ and 3, respectively. (C) Changes in the effective quantum yield of electron flow in PSII induced by the background light and by the 30-s pulse of LL applied in 5.5 min after the onset of background illumination (dashed lines and the bar LL show the position and duration of the localized light pulse).

Our attention was primarily focused on the F' transients induced by localized illumination of a distant cell part (the peak at t ~400 s). From the records similar to Fig. 4B, the kinetics of the effective quantum yield of electron flow in PSII ($\Delta F/F_m'$) was plotted (Fig. 4C). The results reveal a transient drop in $\Delta F/F_m'$ induced by the localized illumination. The F' and F_m' kinetics in Fig. 4B allowed the estimation of quenching coefficients qP and qN, as defined in [26,29], at any instant from the onset of background illumination and the LL pulse. Although direct determination of the parameter F_o' included in equations for qP and qN is usually complicated, F_o' can be conveniently calculated from readily measured fluorescence parameters using a formula derived by Oxborough and Baker [40]. The quenching analysis according to this method revealed that the decrease in qP at the peak of F' response was sixfold larger than that of qN. Hence, the increase in F' and the respective drop in $\Delta F/F_m'$ were caused by the decrease in photochemical quenching (i.e., by Q_A reduction).

It should be pointed out that definite conclusions on the origin of cyclosis-mediated changes in $\Delta F/F_m'$ can be made directly from the results in Fig. 4 without determination of quenching parameters. If the cyclosis-mediated changes in F' were to be caused by non-photochemical quenching (NPQ), they should be smaller than the respective changes in F_m', because F_m' is unaffected by photochemical process (rate constant k_p) whereas F' value is attenuated by photochemical events. With this in mind and considering equal units for F' and F_m' in Fig. 4B, the inspection of this plot shows that the increase in F' in response to cyclosis-mediated signal (the shift ~100 mV in the output voltage of PAM control unit at t ~400 s) was severalfold larger than the concomitant increase in F_m' (<20 mV). This excludes the decrease in NPQ as a possible cause for cyclosis-mediated drop of $\Delta F/F_m'$ in Fig. 4C.

The rate of linear electron transport is proportional to the product of light intensity and the effective quantum yield of PSII photochemistry, $\Delta F/F_m'$. The analyzed cell area remains under constant irradiance from the onset of background illumination (from t ~20 s onward). It may be noted here that the illuminated area is positioned at a distance of 1.5 mm from the point of fluorescence measurements. Similar though delayed changes in fluorescence parameters were observed at distances up to 4.5 mm from the point of illumination, which excludes the increase in light intensity due to light scattering. Hence, the clear drop in $\Delta F/F_m'$ in Fig. 4C at t ~400 s (~10%) indicates the deceleration of electron transport rate. It thus appears that the transported signal is metabolically active and induces temporal retardation of photosynthetic linear electron flow. This slowing down of electron transport in PSII is not surprising considering that the content of oxidized Q_A decreases.

3.4. Cyclosis-mediated F′ transients as a function of preceding light conditions

Since the F' response to LL was absent in dark-adapted chloroplasts, its dependence on the preceding dark and light intervals was of interest. As stated above, a 5-min dark adaptation was followed by the complete disappearance of cyclosis-mediated F' changes; the incubation in darkness for 3 min resulted in strong (by about 80–90%) but incomplete inhibition. Therefore, the cell was dark-adapted for 5 min prior to each measurement. The experimental protocol with an application of a single LL pulse was similar to that illustrated in Fig. 4B. The time $t = 0$ corresponds to the onset of F' recording at the end of a 5-min dark period. At $t = 20$ s continuous background light (whole cell illumination, PFD ~9 μmol m^{-2} s^{-1}) was switched on. After variable lengths of background illumination, a 30-s pulse of localized light was applied at a 1.5-mm distance from the point of fluorescence measurements.

In Fig. 5 (solid symbols) the amplitudes of F' changes induced by localized illumination are plotted against the duration of the background illumination preceding the LL pulse. It is seen that localized lighting applied after short periods of background light (<50 s) produced no F' changes. The amplitude of F' response increased to the plateau with the length of background illumination in the range from 50 to 150 s. Experimental data were approximated with a sigmoid curve.

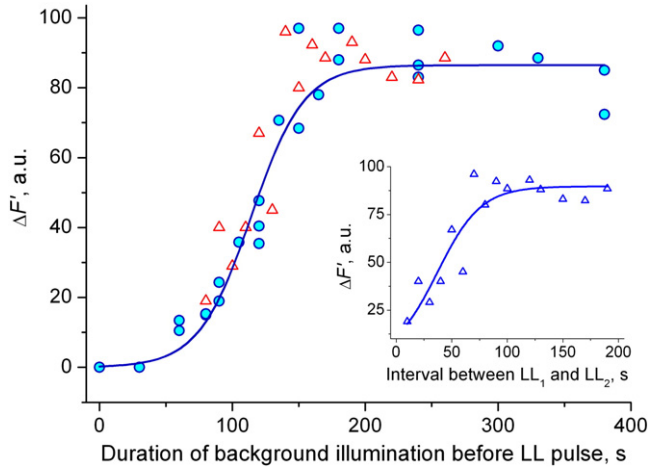

Fig. 5. Amplitude of the F' changes ($\Delta F'$) induced by illumination of a distant cell area (d = 1.5 mm) with a 30-s pulse of LL as a function of duration of background illumination preceding the application of LL pulse. The inset shows the amplitude of $\Delta F'$ induced by the second 30-s pulse of LL (LL_2) plotted against the duration of dark interval separating LL_1 and LL_2. The first pulse of LL (LL_1) was applied in 10 s after the onset of the background light and the second pulse was applied after variable periods from the end of the first pulse. Data points obtained on various cells were normalized to the highest $\Delta F'$ amplitude. Data shown with solid and open symbols were obtained using a single LL pulse protocol (as in Fig. 4B) and a double LL sequence (as in Fig. 4A), respectively.

We wondered if the first pulse of localized illumination (LL_1) in the double-pulse experiments illustrated in Fig. 4A had its own influence on the response induced by the LL_2 pulse. To test this possibility we used the experimental protocol similar to that in Fig. 4A, in which the interval between LL_1 and LL_2 was varied from 10 to 200 s, and examined the extent of F' changes as a function of the interpulse interval (the first 30-s pulse was applied at t = 50 s). The plot thus obtained (Fig. 5, inset) showed a rising branch and a plateau. When these data were plotted against time of the preceding background illumination (the period of 70 s from the onset of background light to the end of LL_1 pulse was taken into account), the data points fell satisfactorily into the plot against the length of preceding background illumination (open symbols in Fig. 5). It means that the induction phenomena in the cell part exposed to weak background light, including the area of fluorescence measurements, were the limiting factor for the development of cyclosis-mediated F' responses. This suggestion seems reasonable because the photosynthetic induction phenomena develop slower at low light than in the cell region exposed to high-intensity localized illumination.

3.5. Dependences of F' changes on the background and localized irradiance

The amplitudes of cyclosis-mediated F' responses to LL were affected by the intensities of background light and localized illumination (Fig. 6). In the absence of background illumination, the LL induced no fluorescence response (data not shown). A small discernible increase in F' was observed at incident light intensities of about 3 μmol m^{-2} s^{-1}. The amplitude of F' changes increased steeply with the background irradiance and reached the highest values at PFD ~10 μmol m^{-2} s^{-1} (Fig. 6A). When the intensities of background light were elevated above this level, the cyclosis-mediated F' response was lowered. Clearly, when the intensity of background light was too low, the chloroplasts of the shaded cell part were insensitive to the propagated signal. On the other hand, at high intensities of background light the signal generated by the pulse of localized light produced little effect because metabolic activities of cell areas exposed to localized and overall illumination were not strikingly different.

The major part of experiments was performed at LL intensity fixed at its maximal level. In addition, we examined the cyclosis-mediated F'

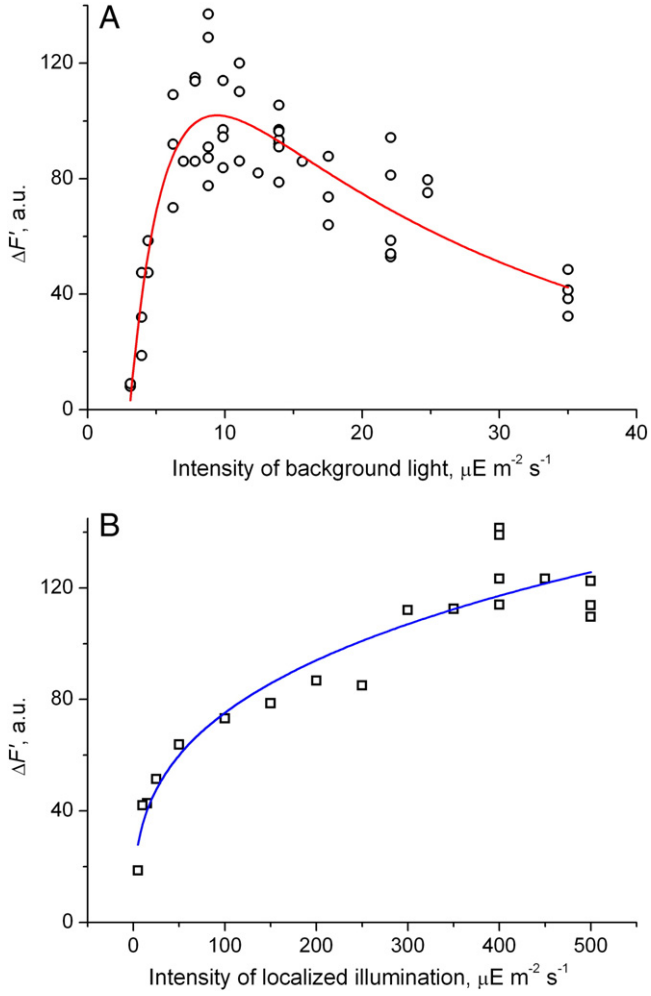

Fig. 6. The amplitude of cyclosis-mediated F' response to a 30-s pulse of localized illumination in a distant cell area as a function of photon flux densities of (A) continuous background light incident on the whole cell and (B) localized illumination applied at a distance of 1.5 mm from the area of fluorescence measurements.

changes at lower intensities of LL. Data points in Fig. 6B show that the F' response approached the saturation at PFD range of 300–500 μmol m^{-2} s^{-1}. The half-maximal amplitude of the F' response was observed upon the tenfold attenuation of LL intensity (at PFD ~50 μmol m^{-2} s^{-1}). The steep portion of the light-response curve was confined to the range of intensities that were equal or less than those of background illumination (photon flux densities <10 μmol m^{-2} s^{-1}). This indicates that the F' changes induced by the distant LL stimulus cannot be considered as a specific response to excess light. It is more likely that the F' signals reflect different physiological levels of photosynthetic metabolism in brightly illuminated and shaded cell parts.

3.6. Role of natural electron carriers on the acceptor side of PSI

The photosynthetic induction phenomena are largely due to the CO_2-dependent electron transport on the acceptor side of PSI [31,33], which activates the enzymes of photosynthetic dark reactions via ferredoxin–thioredoxin reduction (reviewed in [3,12]). It is known that reduction of NADP in dark-adapted leaves does not start immediately after the dark–light transition but occurs after a lag period of several tens of seconds; this delay is determined by photoactivation of ferredoxin–NADP reductase (FNR) that is inactivated after dark incubation (e.g., [33]). The electron transport to NADP can be averted in

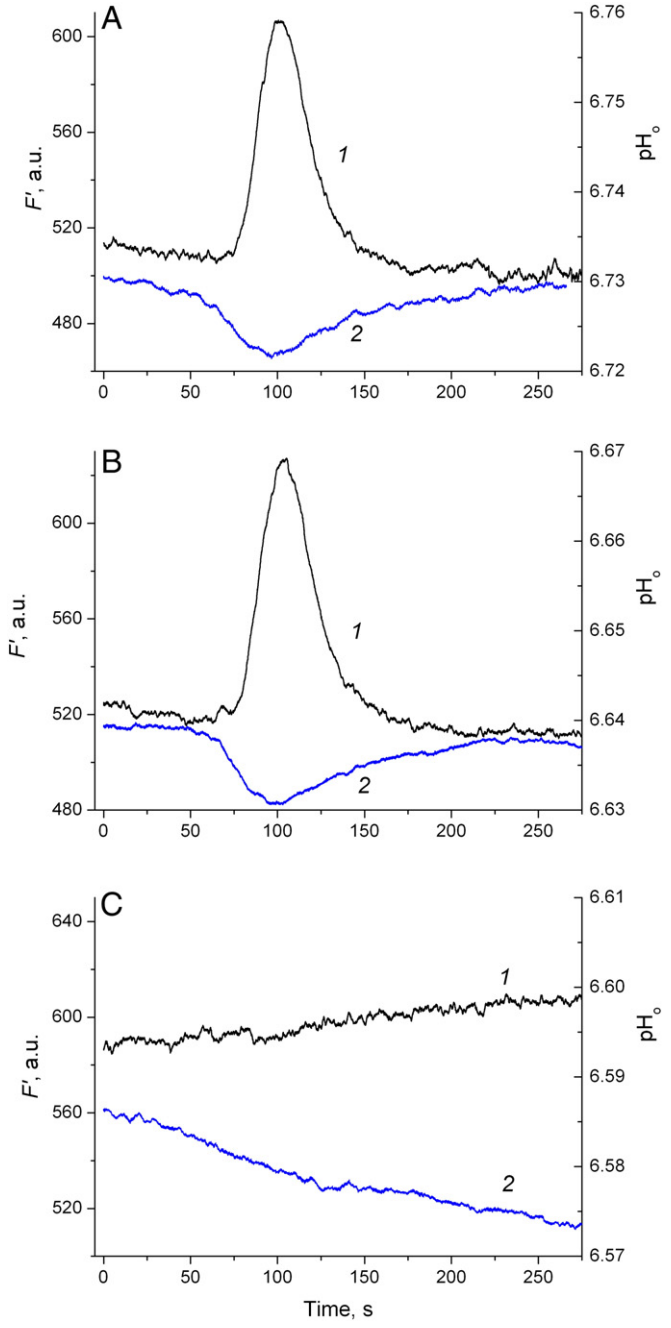

Fig. 7. Elimination of cyclosis-mediated F' fluorescence changes (curves *1*) and the surface pH (pH_o) in the same cell region (curves *2*) after controlled switching of the electron flow on the acceptor side of PSI to oxygen reduction catalyzed by methyl viologen (MV). (A) Cyclosis-mediated F' response accompanied by slight acidification of the apoplast under control conditions, in the absence of MV. Averaged records are presented with $n = 4$ and 2 for $\Delta F'$ and pH_o measurements, respectively. (B) The lack of visible alterations in cyclosis-mediated changes of F' and pH_o after 30-min incubation of the resting cell in the presence of 25 μM MV. Averaged records are presented with $n = 4$ and 3 for $\Delta F'$ and pH_o measurements. (C) Elimination of cyclosis-mediated changes in F' and pH_o after elicitation of a single action potential known to open the membrane barrier for MV permeation and to catalyze electron flow to oxygen. Averaged records are shown ($n = 3$).

the presence of methyl viologen (MV) that redirects electron transport to molecular O_2 as a terminal acceptor.

In this connection, we tested if the cyclosis-mediated F' changes are affected by methyl viologen. Fig. 7 shows the results of simultaneous measurements of fluorescence F' and the surface pH (pH_o) in the same cell area. Under control conditions (Fig. 7A) the standard response of F' (curve *1*) was observed; it was accompanied by a slight decrease in surface pH (formation of acid zone, curve *2*). The addition of MV to the bath medium to a final concentration of 25 μM produced no significant changes in responses of F' and pH_o to localized illumination throughout a 30-min incubation period (Fig. 7B). This is in line with previous reports that MV does not permeate through the plasma membrane of *Chara* and remains inaccessible for chloroplasts, at least in the areas with slightly acid external pH [41]. However, MV was shown to permeate immediately into chloroplasts and switch over the electron transport routes after a single elicitation of the action potential [41,42]. Our present experiments confirm that MV becomes immediately accessible to chloroplasts after a single AP generation. They also show that the replacement of native electron transport with oxygen reduction catalyzed by methyl viologen eliminates the cyclosis-mediated F' and pH_o changes (Fig. 7C). Thus, the induction of fluorescence response to localized lighting in a distant cell part involves the reactions occurring on the donor side of PSI and, probably, the dark reactions of the Calvin–Benson cycle.

The treatment with MV modified also the induction curves of chlorophyll fluorescence (Fig. 8). In the absence of MV the kinetics of F' after dark–light transition comprised the delayed peak at $t \sim 300$ s like that shown in Fig. 4. The addition of 25 μM MV had no immediate effect on the kinetics of F' fluorescence until the elicitation of a single action potential. Thereafter, the MV treatment eliminated the delayed peak of F' (cf. curves *1* and *2* in Fig. 8A). Slow quenching of F_m' observed under control conditions (Fig. 4B, Supplemental Fig. 1C) was replaced with a fast strong (by nearly 30%) quenching of F_m' (Fig. 8B). Strong light-induced quenching of F_m' under low-irradiance illumination is

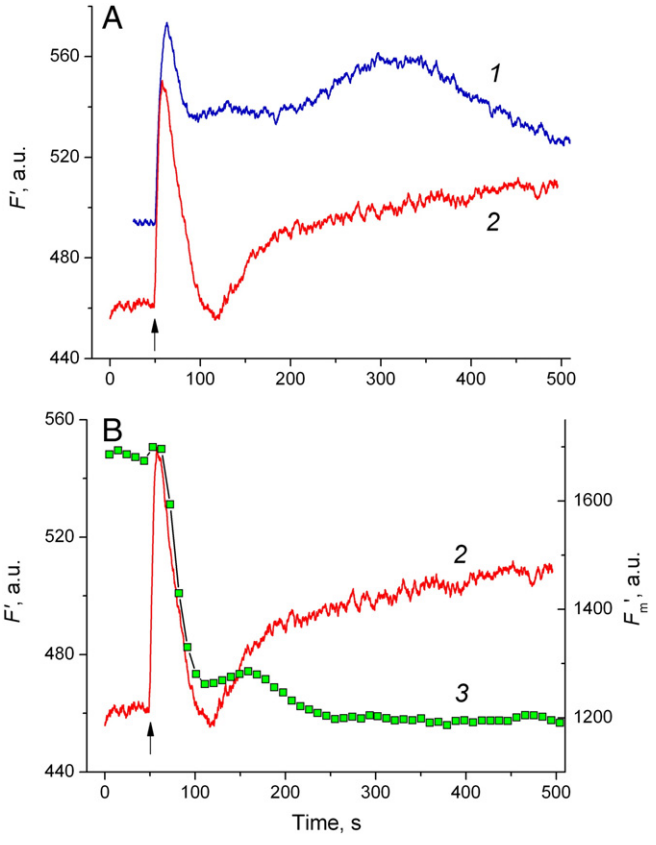

Fig. 8. Effect of methyl viologen (MV) on the induction curves of chlorophyll fluorescence in *Chara* internodal cell upon illumination at PFD of 9 μmol m^{-2} s^{-1}. (A) Induction curves of F' fluorescence under control conditions (*1*) and after incubation with 25 μM MV followed by elicitation of a single action potential (*2*). Arrows in (A) and (B) mark the moments when light was switched on. Note the disappearance of the delayed peak of F' after the MV treatment. (B) Induction curves of F' (*2*) and F_m' (3) after the treatment with 25 μM MV. Note a strong non-photochemical quenching of F_m' induced by low-intensity illumination. Averaged records are shown for $n = 4$ (curve *1*) and $n = 3$ (curves *2*, *3*).

typical of MV-treated cells [41,42]. In the presence of MV the rapid drops in F' and F_m' were coincident, indicating that the drop in F' was largely determined by non-photochemical quenching.

The above results suggest that electron transport pathways beyond PSI are critical for the photoinduction of cyclosis-mediated interactions between distant chloroplasts. The CO_2-dependent electron flow is mediated by FNR whose photoactivation is manifested in transient changes of chlorophyll P700 redox state [33]. Methyl viologen was found to eliminate characteristic FNR-mediated absorbance changes of $P700^+$ at 810 nm in *Chara* cells [42]. Judging from the absorbance changes ΔA_{810}, FNR is activated in *C. corallina* within few seconds of illumination, rather than after illumination periods ~60 s required for the photoinduction of cyclosis-mediated interactions. However, it is not yet known whether photoactivation of FNR proceeds also rapidly at low light intensities. In order to answer this question, we measured absorbance changes of $P700^+$ using a two-step illumination protocol. The first pulse of low-intensity light was followed by a stepwise increase in PFD up to 400 μmol m^{-2} s^{-1}. It is seen in Supplemental Fig. 2A that the first-step illumination at PFD of 80 and 40 μmol m^{-2} s^{-1} induced a characteristic primary oxidation followed by temporary reduction and secondary oxidation of P700, whereas the second pulse of intense light was followed by monotonic increase in ΔA_{810}. By contrast, when the first pulse with PFD of 10 μmol m^{-2} s^{-1} was applied, the ΔA_{810} signal showed no sign of FNR activation, whereas the second light pulse induced the typical multiphase changes assigned to FNR activation. As can be seen in Supplemental Fig. 2B, similar patterns of ΔA_{810} responses were observed after prolongation of the low-intensity light pulse to 5 and 150 s. Hence, at low-light intensities used in this work, photoactivation of FNR is not a rapid process. It is not excluded that a certain threshold light intensity is required for FNR activation.

3.7. Inhibition of cyclosis-mediated F′ changes by diphenyleneiodonium

The role of electron-transport pathways operating on the reducing side of PSI can be also tested with a flavoenzyme inhibitor, diphenyleneiodonium (DPI) that inhibits FNR activity in chloroplasts and cyanobacteria [43,44]. Fig. 9 shows that cyclosis-mediated interactions between distant chloroplasts are reversibly inactivated by dark incubation (Fig. 9A) and irreversibly eliminated after adding 10 μM DPI (Fig. 9B). In 7 min after DPI addition the cyclosis-mediated F' changes were inhibited by nearly 90%, and after 12 min these changes disappeared completely. It is worth noting that this inhibition occurred prior to any significant changes in the background level of F'. After a longer incubation in the presence of DPI (~30 min) the F' fluorescence started to increase, which was accompanied by a substantial drop in $\Delta F/F_m'$ (data not shown). This postponed increase in F' might reflect the increased reduction of intersystem electron carriers after the inhibition of FNR-mediated electron flow on the reducing side of PSI. Strong inhibition of cyclosis-mediated F' changes, which appeared long before the reduction of electron transport chain, may indicate that DPI affects also some other enzyme activities involved in distant communications between chloroplasts, e.g., the activity of NADPH–plastoquinone oxidoreductase [45].

4. Discussion

The results provide new evidence for the direct role of cyclosis in long-distance transmission of photoinduced signals in characean internodes. Such signals may arise in the natural environments under patched illumination of algae with fluctuating light (sunflecks). The emerging patterns of light spots and shaded regions would create the metabolite gradients in the cytoplasm (owing to rapid chloroplast–cytoplasm exchange) and the movement of photosynthetically active metabolites with the cytoplasmic streaming. Thus, the long-distance regulation of photosynthesis is exerted in cell parts remaining under constant irradiance, even in the period when the pulse of LL was

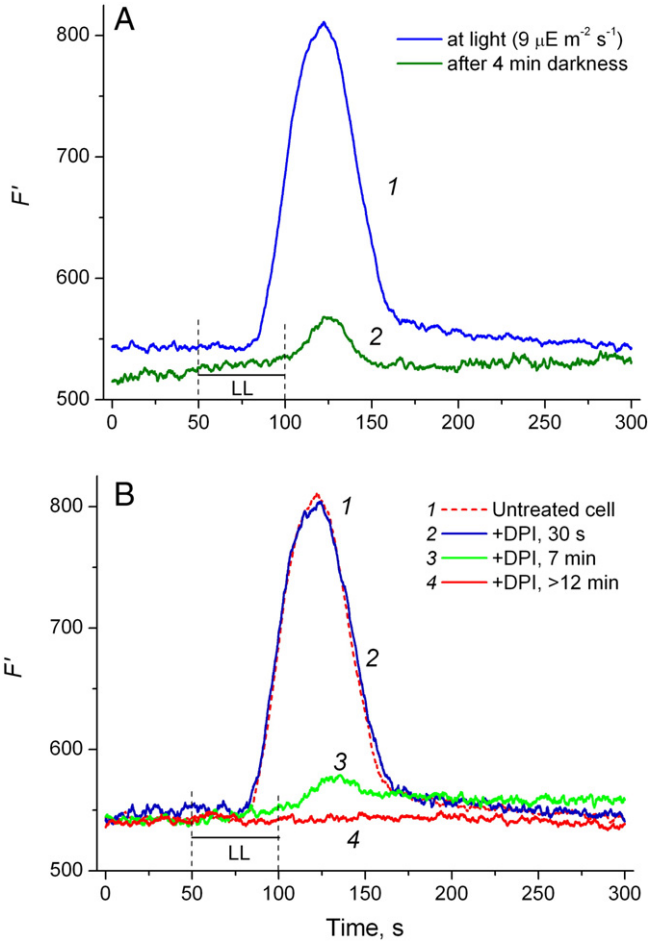

Fig. 9. Reversible suppression of cyclosis-mediated F' fluorescence changes after dark incubation and irreversible inhibition by diphenyleneiodonium (DPI). (A) Cyclosis-mediated F' changes induced by localized illumination of a distant cell region (d = 1.5 mm) at background irradiance of 9 μmol m^{-2} s^{-1} under control conditions (*1*) and after 4-min preincubation in darkness (*2*). Average records are shown (n = 3 and 2 for curves *1* and *2*, respectively). Vertical dashed lines and horizontal bars mark the beginning and end of LL pulse. (B) Inhibition of cyclosis-mediated F' changes after adding 10 μM DPI: (*1*) untreated cell (control conditions); (*2*, *3*, *4*) in 30 s, 7 min, and ≥12 min after the addition of 10 μM DPI. Trace *4* is an average record for n = 2.

extinguished. One functional consequence of such regulation is the facilitated formation of the pH bands on the cell surface ([18] and Fig. 7A).

In a previous study, fluorescence imaging revealed the cyclosis-mediated transfer of H_2O_2 produced in chloroplasts under intense localized illumination [37]. The rapid and reversible increase in F' fluorescence described here seems unrelated to the cytoplasmic flow of H_2O_2, because no release of H_2O_2 from chloroplasts to the streaming cytoplasm was noticed in cell images when the exposure to strong LL was 30 s or shorter, even at the highest intensities of LL. Unlike lateral transfer of H_2O_2, the cyclosis-mediated F' response remained evident at shorter illumination periods (Fig. 2B) and was observed even at low intensities of LL (Fig. 6B). Furthermore, the effects of H_2O_2 on chlorophyll fluorescence and photosynthesis seem to be implemented indirectly, rather than through direct influence of H_2O_2 on the redox state of electron transport carriers [46].

The present study, unlike related works [17,25], was focused on cyclosis-mediated changes in actual fluorescence F'. While changes in the maximal fluorescence F_m' contain information on non-photochemical quenching, large dynamic changes in F' represent a suitable indicator of the reduction–oxidation state of the electron acceptor Q_A in PSII. Other processes, such as development/release of non-photochemical quenching including state transitions may also affect fluorescence F' to a smaller extent. The changes in F' and F_m'

induced by localized illumination of a distant cell area exhibit both shared and distinct properties. There is sufficient evidence that F' and F_m' changes in response to LL are mediated by cytoplasmic streaming (Figs. 1, 3 and Refs. [17,25]). However, the F' kinetics always exhibited the dominant stage of the transient fluorescence increase, whereas the F_m' response comprised the stages of both polarities, with the F_m' quenching stage being particularly large. Apparently, the monitoring of F_m' and F' provides complementary information on the processes related to long-distance propagation of photoinduced signals and on signal perception by chloroplasts.

One possible explanation of the F' transients examined here implies the release of reducing equivalents across the envelope membranes of brightly illuminated chloroplasts, subsequent translocation of reduced agents with the cytoplasmic flow, and the entry of reducing equivalents into the chloroplasts of the shaded regions, where they affect the redox state of electron carriers in the photosynthetic electron transport chain. The rapid exchange of reducing equivalents between the chloroplast stroma and the cytoplasm was emphasized in many studies [3,4,12,13]. The indirect transfer of reduced substances is assisted by the malate/oxaloacetate shuttle and triose-phosphate/phosphoglycerate shuttle. These systems may operate both in the areas of signal generation and in the signal perception regions. The chemical nature of the redox components involved remains unknown. According to the schemes suggested in the literature, accumulation of NADPH in the stroma of illuminated chloroplasts might drive the conversion of stromal oxaloacetate into malate that is exported into the cytosol and reduces the cytoplasmic NAD [4]. In cell areas exposed to dim light, a similar series of backward reactions involving the cytoplasmic NADH transported with the liquid flow would account for the increase in stromal concentration of NADPH.

The increase in the stromal reduction in chloroplasts exposed to dim light, e.g., the supposed increase in NADPH content may promote non-photochemical reduction of plastoquinone by means of NAD(P)H dehydrogenase [13], thus affecting the redox state of Q_A. This notion is supported by observations of non-photochemical NAD(P)H-dependent plastoquinone reduction and enhancement of chlorophyll fluorescence in darkened thylakoid membranes of potato [43] and *Chlamydomonas reinhardtii* [45]. Moreover, the NADPH-dependent increase in fluorescence was strongly inhibited by 10 μM DPI [45], which agrees with data in Fig. 9. The redox poise of NAD(P)H was also reported to have a regulatory effect on intersystem electron transport in intact leaves [47].

As an alternative, we considered the possibility that the increase in stromal reductant (NADPH) may cause photochemical Q_A reduction because of the shortage of oxidized acceptor (NADP) for linear electron flow. Such a restriction of electron transfer from ferredoxin to NADP might result in the reduction of the intersystem carriers, including the quinone acceptor Q_A, and the respective increase in fluorescence F'. The described sequence of events is only possible when electron transport on the acceptor side of PSI is not disconnected from NADP as a terminal electron acceptor. Ample evidence indicates that the electron transport between ferredoxin and NADP is blocked in dark-adapted samples because of the dark inactivation of ferredoxin–NADP reductase [33,48,49]. In the case of disconnection of electron transport from ferredoxin to NADP, the increase in the stromal NADPH concentration may have little effect on photosynthetic electron flow.

These two alternative interpretations for F' dependence on the stromal NADPH – non-photochemical PQ reduction and the increase in photochemical PQ reduction under shortage of NADP as a terminal electron acceptor – imply different mechanisms underlying the photoinduction of cyclosis-mediated interactions. The priority in explanation is given to the ferredoxin–thioredoxin system that activates in the light the stromal NADP–malate dehydrogenase involved in the transport of reducing equivalents by the malate shuttle across the chloroplast envelope [3,4]. In this case the photoinduction of cyclosis-mediated interactions between distant chloroplasts is mainly limited by the transport of reductants across the chloroplast envelopes both in the source and recipient cell parts.

The alternative notion of photochemical PQ reduction under elevated stromal NADPH considers the photoinduction of cyclosis-mediated interactions in terms of FNR photoactivation that opens the pathway for electron transfer between ferredoxin and NADP, thus making electron flow sensitive to the content of stromal NADPH. One argument against this view is that the activation of FNR in *Chara* is completed within 1 s at moderate and high irradiances (Supplemental Fig. 2), which would be inconsistent with the photoinduction periods ~50 s documented in Figs. 4 and 5. At low irradiance (~10 μmol m^{-2} s^{-1}) no FNR activation was observed in the time range of seconds and tens of seconds; however, its activation at longer exposures in low light remained unproven. The role of FNR in cyclosis-mediated interactions of chloroplasts is partly supported by elimination of F' response to LL by DPI, a FNR inhibitor (Fig. 9). Nevertheless, the F' response to LL disappeared prior to any discernible increase in the background level of F' fluorescence, which may indicate the involvement of other DPI-sensitive processes.

The divergence of electron transport pathways from ferredoxin to various acceptors, including NADP, thioredoxin, and the artificial redox mediator MV, implies the competitive relations between these pathways. The increasing reduction of the thioredoxin pool increases the activation state of NADP-malate dehydrogenase that controls the malate valve [50]. One may suppose that, at subthreshold irradiances insufficient for the outflow of electrons through FNR to NADP, the ferredoxin–thioredoxin system activates the light-dependent stages in cyclosis-mediated interactions between distant chloroplasts. From this point of view, the light-intensity plot shown in Fig. 6A may correspond to the profile of the activation of FNR on the acceptor side of PSI. In consistency with this notion, free outflow of electrons on the acceptor side of PSI in the presence of MV or at elevated irradiance in the absence of MV prevents the photoinduction of a reduced PQ pool.

The present results reveal some additional features of cyclosis-mediated transmission of photoinduced signals. In resting cells where cytoplasmic streaming proceeds at a constant rate, the width of the F' response at a half-maximal height increased in proportion to the duration of localized illumination (Fig. 2A). The temporal arrest of streaming delayed and extended the development of individual stages of the F' response to LL (Fig. 3). Depending on the precise moment of the AP-elicited streaming cessation, either the frontal or rear slopes of the response were extended. During the period of complete cessation of streaming, the signaling substance may move from its location only by diffusion. However, no significant increase in F' was noted by the end of a 30-s period corresponding to full stoppage of streaming, when the action potential was elicited simultaneously with the onset of localized illumination (Fig. 3A, curve *2*). Clearly, diffusion is an ineffective means of signal transmission for millimeter distances. When the AP and streaming cessation were elicited during the passage of a signaling substance across the region of fluorescence measurement, the fluorescence F' showed a slow decline after reaching the peak (Fig. 3B). The origin of this slow decline might be complex and include the metabolic decreases in the cytoplasmic and stromal levels of the signaling substance as well as its diffusion. It is tempting to develop in future studies a simulation model that could account for the dynamic behavior of cyclosis-mediated fluorescence changes after interruption of streaming at any arbitrary moment before, during, or after the localized illumination. Such a simulation may be helpful to comprehend the dynamics of photosynthesis in fluctuating light under natural environmental conditions.

Summing up, the results indicate that reducing equivalents produced in the stroma of illuminated chloroplasts are likely conveyed to the streaming cytoplasm and transported with the flow for long distances, whereas subsequent shuttling of redox substances across the envelope membrane in chloroplasts exposed to dim light results in the transient reduction of stromal components and intersystem carriers

in the photosynthetic electron transport chain. Furthermore, the terminal steps in the considered sequence of events seem to depend crucially on electron transport in the acceptor part of PSI, which is sensitive to methyl viologen and the flavoenzyme inhibitor of FNR and NAD(P)H–plastoquinone reductase.

Supplementary data to this article can be found online at http://dx.doi.org/10.1016/j.bbabio.2015.01.004.

Conflict of interests

The authors declare that they have no conflict of interest.

Acknowledgments

This work was supported by the Russian Foundation for Basic Research, project no. 13-04-00158. We would like to acknowledge the reviewers for their positive and constructive remarks.

References

[1] U.-I. Flügge, H.W. Heldt, Metabolite translocators of the chloroplast envelope, Annu. Rev. Plant Physiol. Plant Mol. Biol. 42 (1991) 129–144.
[2] A.P.M. Weber, R. Schwacke, U.-I. Flügge, Solute transporters of the plastid envelope membrane, Annu. Rev. Plant Biol. 56 (2005) 133–164.
[3] C.H. Foyer, G. Noctor, Redox regulation in photosynthetic organisms: signaling, acclimation, and practical implications, Antioxid. Redox Signal. 11 (2009) 861–905.
[4] M. Taniguchi, H. Miyake, Redox-shuttling between chloroplast and cytosol: integration of intra-chloroplast and extra-chloroplast metabolism, Curr. Opin. Plant Biol. 15 (2012) 1–9.
[5] W.L. Araújo, A. Nunes-Nesi, A.R. Fernie, On the role of plant mitochondrial metabolism and its impact on photosynthesis in both optimal and sub-optimal growth conditions, Photosynth. Res. 119 (2014) 141–156.
[6] K. Noguchi, K. Yoshida, Interaction between photosynthesis and respiration in illuminated leaves, Mitochondrion 8 (2008) 87–99.
[7] A.S. Raghavendra, K. Padmasree, Beneficial interactions of mitochondrial metabolism with photosynthetic carbon metabolism, Trends Plant Sci. 8 (2003) 546–553.
[8] K. Padmasree, L. Padmavathi, A.S. Raghavendra, Essentiality of mitochondrial oxidative metabolism for photosynthesis: optimization of carbon assimilation and protection against photoinhibition, Crit. Rev. Biochem. Mol. Biol. 37 (2002) 71–119.
[9] F.A. Busch, T.L. Sage, A.B. Cousins, R.F. Sage, C_3 plants enhance rates of photosynthesis by reassimilating photorespired and respired CO_2, Plant Cell Environ. 36 (2013) 200–212.
[10] M.S. Islam, Y. Niwa, S. Takagi, Light-dependent intracellular positioning of mitochondria in *Arabidopsis thaliana* mesophyll cells, Plant Cell Physiol. 50 (2009) 1032–1040.
[11] I. Foissner, Microfilaments and microtubules control the shape, motility, and subcellular distribution of cortical mitochondria in characean internodal cells, Protoplasma 224 (2004) 145–157.
[12] T. Kopczewski, E. Kuźniak, Redox signals as a language of interorganellar communication in plant cells, Cent. Eur. J. Biol. 8 (2013) 1153–1163.
[13] P.J. Nixon, Chlororespiration, Philos. Trans. R. Soc. B 355 (2000) 1541–1547.
[14] A.A. Bulychev, Membrane excitation and cytoplasmic streaming as modulators of photosynthesis and proton flows in Characean cells, in: A.G. Volkov (Ed.), Plant Electrophysiology: Methods and Cell Electrophysiology, Springer, Berlin, 2012, pp. 273–300.
[15] M.J. Beilby, M.A. Bisson, pH banding in charophyte algae, in: A.G. Volkov (Ed.), Plant Electrophysiology: Methods and Cell Electrophysiology, Springer, Berlin, 2012, pp. 247–271.
[16] A.A. Bulychev, S.O. Dodonova, Role of cyclosis in asymmetric formation of alkaline zones at the boundaries of illuminated region in *Chara* cells, Russ. J. Plant Physiol. 58 (2011) 233–237.
[17] A.A. Bulychev, S.O. Dodonova, Effects of cyclosis on chloroplast–cytoplasm interactions revealed with localized lighting in Characean cells at rest and after electrical excitation, Biochim. Biophys. Acta 1807 (2011) 1221–1230.
[18] S.O. Dodonova, A.A. Bulychev, Cyclosis-related asymmetry of chloroplast–plasma membrane interactions at the margins of illuminated area in *Chara corallina* cells, Protoplasma 248 (2011) 737–749.
[19] W.F. Pickard, The role of cytoplasmic streaming in symplastic transport, Plant Cell Environ. 26 (2003) 1–15.
[20] T. Shimmen, The sliding theory of cytoplasmic streaming: fifty years of progress, J. Plant Res. 120 (2007) 31–43.
[21] T. Shimmen, E. Yokota, Cytoplasmic streaming in plants, Curr. Opin. Cell Biol. 16 (2004) 68–72.
[22] J. Verchot-Lubicz, R.E. Goldstein, Cytoplasmic streaming enables the distribution of molecules and vesicles in large plant cells, Protoplasma 240 (2010) 99–107.
[23] R.E. Williamson, C.C. Ashley, Free Ca^{2+} and cytoplasmic streaming in the alga *Chara*, Nature 296 (1982) 647–651.
[24] M. Tazawa, M. Kikuyama, Is Ca^{2+} release from internal stores involved in membrane excitation in characean cells? Plant Cell Physiol. 44 (2003) 518–526.
[25] A.A. Bulychev, A.V. Alova, A.B. Rubin, Propagation of photoinduced signals with the cytoplasmic flow along characean internodes: evidence from changes in chloroplast fluorescence and surface pH, Eur. Biophys. J. 42 (2013) 441–453.
[26] U. Schreiber, Pulse-amplitude-modulation (PAM) fluorometry and saturation pulse method: an overview, in: G.C. Papageorgiou, Govindjee (Eds.), Chlorophyll *a* Fluorescence: A Signature Of Photosynthesis, Springer, Dordrecht, 2004, pp. 279–319.
[27] N.R. Baker, Chlorophyll fluorescence: a probe of photosynthesis in vivo, Annu. Rev. Plant Biol. 59 (2008) 89–113.
[28] Govindjee, Chlorophyll *a* fluorescence: a bit of basics and history, in: G.C. Papageorgiou, Govindjee (Eds.), Chlorophyll *a* Fluorescence. A Signature of Photosynthesis, Springer, Dordrecht, 2004, pp. 1–42.
[29] O. van Kooten, J.F.H. Snel, The use of chlorophyll fluorescence nomenclature in plant stress physiology, Photosynth. Res. 25 (1990) 147–150.
[30] C.-H. Goh, U. Schreiber, R. Hedrich, New approach of monitoring changes in chlorophyll *a* fluorescence of single guard cells and protoplasts in response to physiological stimuli, Plant Cell Environ. 22 (1999) 1057–1070.
[31] D.A. Walker, Photosynthetic induction phenomena and the light activation of ribulose diphosphate carboxylase, New Phytol. 72 (1973) 209–235.
[32] A.A. Bulychev, Different kinetics of membrane potential formation in dark-adapted and preilluminated chloroplasts, Biochim. Biophys. Acta 766 (1984) 647–652.
[33] J. Harbinson, C.L. Hedley, Changes in P-700 oxidation during the early stages of the induction of photosynthesis, Plant Physiol. 103 (1993) 649–660.
[34] N. Kamiya, Protoplasmic Streaming, Springer, Wien, 1959.
[35] A.A. Bulychev, N.A. Kamzolkina, Effect of action potential on photosynthesis and spatially distributed H^+ fluxes in cells and chloroplasts of *Chara corallina*, Russ. J. Plant Physiol. 53 (2006) 1–9.
[36] A.A. Bulychev, A.A. Cherkashin, A.B. Rubin, Dependence of chlorophyll P700 redox transients during the induction period on the transmembrane distribution of protons in chloroplasts of pea leaves, Russ. J. Plant Physiol. 57 (2010) 20–27.
[37] A. Eremin, A.A. Bulychev, M.J.B. Hauser, Cyclosis-mediated transfer of H_2O_2 elicited by localized illumination of *Chara* cells and its relevance to the formation of pH bands, Protoplasma 250 (2013) 1339–1349.
[38] G.C. Papageorgiou, M. Tsimilli-Michael, K. Stamatakis, The fast and slow kinetics of chlorophyll *a* fluorescence induction in plants, algae and cyanobacteria: a viewpoint, Photosynth. Res. 94 (2007) 275–290.
[39] A. Yamagishi, K. Satoh, S. Katoh, Fluorescence induction in chloroplasts isolated from the green alga *Bryopsis maxima* III. A fluorescence transient indicating proton gradient across the thylakoid membrane, Plant Cell Physiol. 19 (1978) 17–25.
[40] K. Oxborough, N.R. Baker, Resolving chlorophyll *a* fluorescence images of photosynthetic efficiency into photochemical and non-photochemical components — calculation of *qP* and *Fv′/Fm′* without measuring *Fo′*, Photosynth. Res. 54 (1997) 135–142.
[41] N.A. Krupenina, A.A. Bulychev, U. Schreiber, Chlorophyll fluorescence images demonstrate variable pathways in the effects of plasma membrane excitation on electron flow in chloroplasts of *Chara* cells, Protoplasma 248 (2011) 513–522.
[42] A.A. Bulychev, N.A. Krupenina, Facilitated permeation of methyl viologen into chloroplasts in situ during electric pulse generation in excitable plant cell membranes, Biochem. (Moscow) Suppl. Series A: Membr. Cell Biol. 2 (2008) 387–394.
[43] S. Corneille, L. Cournac, G. Guedeney, M. Havaux, G. Peltier, Reduction of the plastoquinone pool by exogenous NADH and NADPH in higher plant chloroplasts: characterization of a NAD(P)H–plastoquinone oxidoreductase activity, Biochim. Biophys. Acta 1363 (1998) 59–69.
[44] H. Koike, M.R. Islam, K. Satoh, Investigation of the function of a *nuoE* homologue, *sll1220* in *Synechocystis* sp. PCC6803 by means of mutagenesis, in: J.F. Allen, E. Gantt, J.H. Golbeck, B. Osmond (Eds.), Photosynthesis. Energy From the Sun: 14th International Congress on Photosynthesis, Springer, Dordrecht, 2008, pp. 623–626.
[45] F. Mus, L. Cournac, V. Cardettini, A. Caruana, G. Peltier, Inhibitor studies on non-photochemical plastoquinone reduction and H_2 photoproduction in *Chlamydomonas reinhardtii*, Biochim. Biophys. Acta 1708 (2005) 322–332.
[46] B. Ivanov, M. Kozuleva, M. Mubarakshina, Oxygen metabolism in chloroplast, in: P. Bubulya (Ed.), Cell Metabolism — Cell Homeostasis and Cell Response, InTech, Rijeka, Croatia, 2012, pp. 39–72.
[47] S. Hald, B. Nandha, P. Gallois, G.N. Johnson, Feedback regulation of photosynthetic electron transport by NADP(H) redox poise, Biochim. Biophys. Acta 1777 (2008) 433–440.
[48] K. Satoh, Mechanism of photoactivation of electron transport in intact *Bryopsis* chloroplasts, Plant Physiol. 70 (1982) 1413–1416.
[49] D. Lazár, G. Schansker, Models of chlorophyll *a* fluorescence transients, in: A. Laisk, L. Nedbal, Govindjee (Eds.), Photosynthesis in silico: Understanding Complexity From Molecules to Ecosystems, Springer, Dordrecht, 2009, pp. 85–123.
[50] C.H. Foyer, J. Neukermans, G. Queval, G. Noctor, J. Harbinson, Photosynthetic control of electron transport and the regulation of gene expression, J. Exp. Bot. 63 (2012) 1637–1661.